

# dc Conductivity, Optical Absorption, and Photoconductivity of Amorphous Arsenic Telluride Films

K. WEISER AND M. H. BRODSKY

IBM Research Division, Yorktown Heights, New York 10598

(Received 8 September 1969)

Conductivity, optical absorption, and photoconductivity experiments on amorphous  $\text{As}_2\text{Te}_3$  films are described. The films were prepared by condensation of the vapor on a cooled substrate. Over the temperature range from about 200 to 400°K, the conductivity is of the form  $\sigma = \sigma_0 e^{-\Delta E/kT}$ , with  $\sigma_0 = 600 \Omega^{-1} \text{cm}^{-1}$  and  $\Delta E = 0.4 \text{ eV}$ . This result is interpreted in terms of a "conductivity gap" of 0.8 eV. An analysis of the preexponential factor yields an average mobility between about 0.3 and 5  $\text{cm}^2/\text{V sec}$ , suggesting that the "mobility edges" which are responsible for the conductivity gap are on the borderline between localized and delocalized states. An "optical gap" is derived from a treatment of the optical-absorption data which suggests that for energies well above the conductivity gap the density of valence and conduction-band states have a parabolic dependence on energy. The optical gap of 0.95–0.98 eV is the energy difference between the edges of these parabolic states. Photoconductivity measurements indicate that the room-temperature lifetime is less than 50 nsec. These measurements provide an estimate of 0.3  $\text{cm}^2/\text{V sec}$  for the lower limit of the mobility of carriers. The photoconductivity data also show the presence of trapping states.

## I. INTRODUCTION

**A**MORPHOUS solids are of considerable interest to solid-state physics because of the intriguing question of the relation between electronic properties and disorder. Early work in the field has been discussed in a review article by Ioffe and Regel.<sup>1</sup> More recent surveys both of theory and experiments can be found in Gubanov's book<sup>2</sup> and in several papers by Mott.<sup>3–5</sup> There appears to be widespread agreement that if, for a given material, the short-range order is the same in the amorphous state as in the crystalline state, some basic features of the electronic properties of the crystalline state are preserved. In particular, it appears that "pseudogaps" exist, similar to forbidden gaps in crystalline solids. The difference is that here the density of electronic states is very low rather than zero as in the case of crystals. Figure 1 is a schematic diagram for an amorphous "intrinsic" semiconductor, i.e., a material in which the Fermi level  $E_F$  is approximately in the middle of a pseudogap. The significance of the conductivity edges  $E_c^n$  and  $E_c^p$  and of the optical gap  $E_G$  will be described below. In this generally accepted model, it is further assumed that the states well within the pseudogap are localized, in the sense that the wave functions fall off exponentially with distance from a given point in real space.<sup>3</sup> States which are well removed in energy from the pseudogap, however, are believed to be non-localized. The transition region, in which both types of states may be present in comparable densities, has been discussed by Banyai.<sup>6</sup> In the localized states, conduction can occur by hopping, i.e., by phonon-assisted transitions between energetically similar states.<sup>3,5</sup> Even for the delocalized states, the conduction mechanism differs from that in crystals because of the importance of dis-

order scattering. The theory is complicated because the electrons are no longer described by Bloch waves. Nevertheless, estimates of the mobility of carriers in the delocalized states have been made, and they yield estimates of mean free paths of many lattice spacings if one assumes a thermal velocity for the carriers.<sup>5</sup>

If the Fermi level lies within the pseudogap, both hopping and conduction via delocalized states will occur, and one can immediately predict their relative importance in different temperature ranges. At very low temperatures, the occupation probability of the delocalized states is negligible and therefore hopping must predominate. At very high temperatures, one would expect conduction via the delocalized states to predominate in view of their much higher mobility. A very similar situation exists, of course, in crystalline semiconductors containing donor and acceptor impurities with levels within the forbidden gap.<sup>7</sup> Conductivity measurements over a wide temperature range are, thus, an obvious first step in the study of amorphous solids. Further insight into the density and the character of the states are obtain-

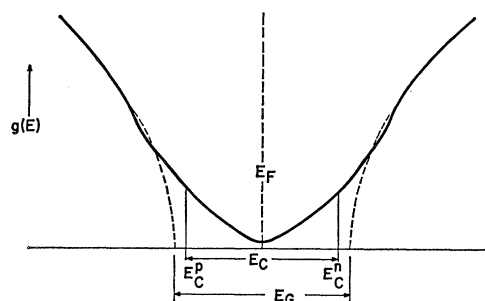


FIG. 1. Density of states versus energy for model employed.  $E_G$  is an optical energy gap obtained by extrapolating high-energy absorption data.  $E_C$  is a conductivity gap obtained from the temperature dependence of the conductivity.

<sup>1</sup> A. F. Ioffe and A. R. Regel, *Progr. Semicond.* **4**, 239 (1960).  
<sup>2</sup> A. I. Gubanov, *Quantum Electron Theory of Amorphous Semiconductors* (Consultants Bureau, New York, 1965).

<sup>3</sup> N. F. Mott, *Rev. Mod. Phys.* **40**, 677 (1968).

<sup>4</sup> N. F. Mott, *J. Non-Cryst. Solids* **1**, 1 (1968).

<sup>5</sup> N. F. Mott, *Phil. Mag.* **19**, 835 (1969).

<sup>6</sup> L. Banyai, *Physique des Semiconducteurs* (Dunod Cie., Paris, 1964), p. 417.

<sup>7</sup> H. Fritzsche and M. Cuevas, *Phys. Rev.* **119**, 1238 (1960).

able from optical absorption and photoconductivity measurements.

In this paper, we report the results of measurements on films of amorphous arsenic telluride ( $\text{As}_2\text{Te}_3$ ). This material was chosen for two reasons. In the first place, it is the least studied of the amorphous chalcogenides, an important class of amorphous semiconductors, which exhibit a wide range of semiconducting properties ordinarily associated with the crystalline phase. Second, glasses containing As and Te plus other constituents have recently come into prominence because of their switching and memory properties.<sup>8-10</sup> Chalcogenide glasses, mainly  $\text{As}_2\text{S}_3$ ,  $\text{As}_2\text{Se}_3$ , and solutions of the latter with  $\text{As}_2\text{Te}_3$  and  $\text{Sb}_2\text{Se}_3$ , have been studied quite extensively over the last several years, particularly by Kolomiets and collaborators,<sup>11-15</sup> by British investigators,<sup>16-18</sup> and by others.<sup>19-22</sup>  $\text{As}_2\text{Te}_3$  has hardly been studied at all because of the difficulty of obtaining it in an amorphous form from the melt. Other chalcogenides, particularly  $\text{As}_2\text{Se}_3$ , can be obtained as a glass by cooling the melt at a conventional rate. To obtain amorphous  $\text{As}_2\text{Te}_3$ , however, it is necessary to quench the melt by especially fast techniques.<sup>23</sup> The most convenient method to prepare the material is by vapor condensation, resulting in thin films, as in the study reported here. This technique was employed by Adrieviskii *et al.*,<sup>24</sup> who carried out electron diffraction studies of these films, and by Rockstad,<sup>25</sup> who studied both dc and ac conductivity and also obtained optical absorption data.

Chalcogenide glasses are characterized by intrinsic semiconductor behavior in the sense that the resistivity increases exponentially with inverse temperature over a wide temperature range. From such behavior in a crystalline semiconductor, one would obtain an activation

energy which corresponds to one-half the energy gap at absolute zero. In an amorphous semiconductor it is assumed that no sharp band edges exist (Fig. 1), and, thus, the interpretation of this activation energy is no longer obvious. Attempts have been made<sup>11,17</sup> to correlate this energy with gaps obtained from optical absorption and photoconductivity data, but interpretation of such data has been ambiguous and often arbitrary. One purpose of this paper is to reexamine the correlation between the energy gap obtained from the electrical data and the gap derivable from optical measurements. We conclude that the two energies are similar but that there is no reason to expect them to be identical. We also show that by making absolute photoconductivity measurements and by studying the time dependence of the photosignal it is possible to obtain insight into the nature of the states near the energy at which the photocarriers make their main contribution to the conductivity.

We report our experimental procedure and results in Sec. II and we interpret the data in Sec. III. In Sec. IV, we summarize the main results of the paper.

## II. EXPERIMENTAL PROCEDURE AND RESULTS

### A. Preparation of Samples

Samples were prepared by condensing the vapor obtained by electron-beam heating of  $\text{As}_2\text{Te}_3$  ingots. These ingots were prepared by reacting the constituents in evacuated sealed quartz tubes at several hundred degrees above the melting point and then cooling the melt to room temperature.<sup>26</sup> A portion of the ingot was then cast into the shape of the hearth of an electron-beam evaporator assembly. The assembly was part of a "dry" high vacuum system, i.e., a system using only sorption, Ti sublimation, and ion pumps. After evacuating the system to about  $10^{-7}$  Torr the material was heated by electron-beam bombardment, and the vapor condensed on a substrate, usually 0.010-in.-thick sapphire, cooled to liquid-nitrogen temperature. In a number of instances, chemical analysis was performed to determine the composition of the condensate, and it was found to be stoichiometric within the accuracy of the analysis<sup>27</sup> which was estimated at no better than 10%. X-ray or electron-diffraction examination of representative films showed no evidence of crystallinity.

The film thicknesses studied was limited to the rather narrow range of 2000–5000 Å. The lower limit was set somewhat arbitrarily by a desire to prevent pinholes. The upper limit was set by the observation that deposits exceeding this thickness tended to crystallize near the surface away from the substrate. The film thickness during the deposition was followed by a Sloan quartz crystal thickness monitor. Typical deposition rates of 400 Å/sec were used and no attempt was made to study

<sup>8</sup> A. D. Pearson, J. F. Dewald, W. R. Northover, and W. F. Peck, Jr., in *Advances in Glass Technology* (Plenum Publishing Corp., New York, 1963), Vol. II, 145.

<sup>9</sup> D. L. Eaton, *J. Am. Ceram. Soc.* **47**, 554 (1964).

<sup>10</sup> S. R. Ovshinsky, *Phys. Rev. Letters* **21**, 1450 (1968).

<sup>11</sup> B. T. Kolomiets, *Phys. Status Solidi* **7**, 359 (1964); **7**, 713 (1964).

<sup>12</sup> B. T. Kolomiets and Yu V. Rukhlyader, *Fiz. Tverd. Tela* **8**, 2762 (1966) [English transl.: *Soviet Phys.—Solid State* **8**, 2201 (1967)].

<sup>13</sup> M. L. Belle, B. T. Kolomiets, and B. V. Pavlov, *Soviet Phys.—Semicond.* **2**, 1210 (1969).

<sup>14</sup> T. N. Vengal and B. T. Kolomiets, *Zh. Tekhn. Fiz.* **27**, 2484 (1957) [English transl.: *Soviet Phys.—Tech. Phys.* **2**, 2314 (1957)].

<sup>15</sup> B. T. Kolomiets, T. N. Mamontova, and V. V. Negreskul, *Phys. Status Solidi* **27**, K15 (1968).

<sup>16</sup> A. E. Owen, N. Clare, and S. Frank, in *Proceedings of the Conference on Low Mobility Solids*, Sheffield, 1966 (unpublished).

<sup>17</sup> J. T. Edmond, *Brit. J. Appl. Phys.* **17**, 979 (1966).

<sup>18</sup> J. C. Male, *Brit. J. Appl. Phys.* **18**, 1543 (1967).

<sup>19</sup> H. L. Uphoff and H. J. Healy, *J. Appl. Phys.* **32**, 950 (1961).

<sup>20</sup> M. D. Coutts and E. R. Levin, *J. Appl. Phys.* **38**, 4039 (1967).

<sup>21</sup> A. Efstrathion and E. R. Levin, *J. Opt. Soc. Am.* **58**, 373 (1968).

<sup>22</sup> N. S. Platakis, H. C. Gatos, and V. Sadagopan, *J. Electrochem. Soc.* **116**, 1436 (1969).

<sup>23</sup> V. Sadagopan (unpublished).

<sup>24</sup> A. I. Andrieviskii, I. D. Nabitovich, and Kristallografiya **6**, 662 (1961) [English transl.: *Soviet Phys.—Crist.* **6**, 534 (1962)].

<sup>25</sup> H. K. Rockstad, *J. Non-Cryst. Solids* (to be published).

<sup>26</sup> We are indebted to J. Kucza and J. Scardefield of this laboratory for preparing these ingots.

<sup>27</sup> B. Gilbert (unpublished).

the effect, if any, of varying these rates on the properties. After completion of the run, the film thickness was determined by measuring Tolansky fringes with a Sloan Angstrom meter.

The samples used for the measurements of electrical conductivity, optical absorption, and photoconductivity were deposited simultaneously, using a mask with appropriate cutouts; their shapes and dimensions are indicated in the inserts of Figs. 2 and 5. Metal electrodes were evaporated on the samples in a vacuum of about  $10^{-6}$  Torr. Care was taken to shield the amorphous film from the radiation given off by the metal source until the latter reached the temperature at which evaporation proceeded at a convenient rate of typically  $75 \text{ \AA/sec}$ . The shutter was then opened and electrodes of about  $1500 \text{ \AA}$  thickness were deposited. For the four probe electrical measurements on the samples of Fig. 2, the nature of the electrical contacts did not matter; both Al and Au were used though it was found that the former makes high-resistance contacts. For the photoconductivity samples it was important to use low-resistance contacts, and it was found that Au was satisfactory for this purpose.

### B. dc Electrical Conductivity between 200 and 400°K

In Fig. 2, we plot the dc electrical conductivity of two typical samples between 220 and 330°K. The current-voltage relation was measured by using Keithly 602 electrometers for both voltage and current measurements. All the data were obtained at sufficiently low fields, typically  $10 \text{ V/cm}$ , to avoid non-Ohmic effects. The measurements were carried out with the samples attached to a copper block which could be cooled below or heated above room temperature. We ascertained that the temperature difference between the film and the copper block was less than about  $1^\circ\text{C}$ . The data points were averaged between those obtained with increasing

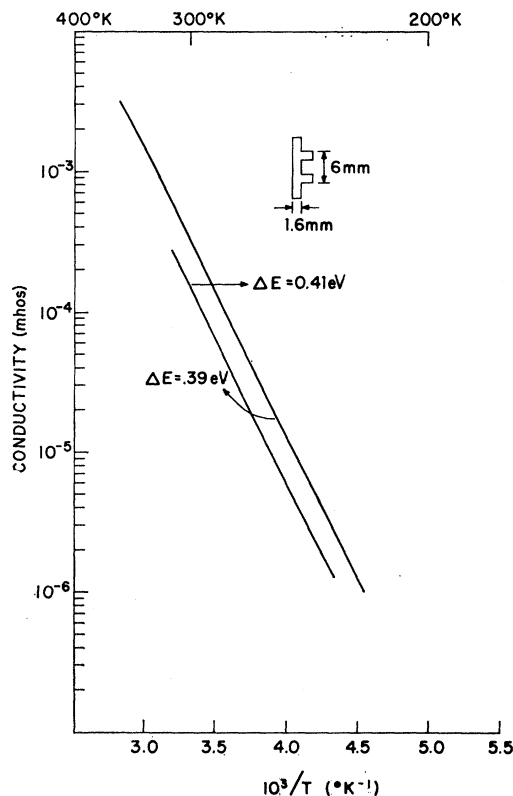
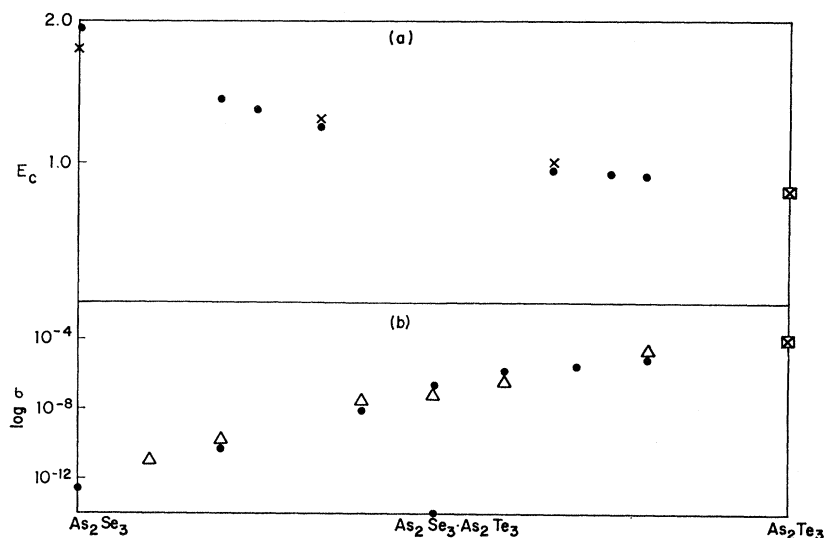


FIG. 2. dc conductivity versus inverse temperature. The curves yield activation energies of 0.41 and 0.39 eV, respectively.

and decreasing temperatures though no significant hysteresis was found. In fact, it should be pointed out that the films were stable upon prolonged storage, i.e., several weeks. The lower temperature limit for these measurements was determined by leakage problems when the sample resistance exceeded approximately  $10^{11} \Omega$ . The upper limit was set by the onset of devitrification

FIG. 3. (a) Conductivity gap and (b) room-temperature conductivity of the  $\text{As}_2\text{Se}_3$ - $\text{As}_2\text{Te}_3$  system.  $\Delta$ , Uphoff and Healy (Ref. 19);  $\bullet$ , Vengel and Kolomiets (Ref. 15);  $\times$ , Edmond (Ref. 17);  $\boxtimes$ , this work.



somewhere between 400 and 450°K, which manifested itself by a five order of magnitude decrease in resistivity.

It is seen from Fig. 2 that the conductivity depends exponentially on temperature with an activation energy  $\Delta E$  of  $0.40 \pm 0.02$  eV. Some samples showed a slight decrease in slope, less than 10%, at low temperatures but because of the leakage problem mentioned earlier it is probable that this drop is not real.

The average room-temperature resistivity found by us is in agreement with that reported by Rockstad.<sup>25</sup> The resistivity and the activation energy should also be compared to those obtained by extrapolating the data for  $\text{As}_2\text{Se}_3\text{-As}_2\text{Te}_3$  glassy solutions investigated by Uphoff and Healy,<sup>19</sup> by Edmonds,<sup>17</sup> and by Vengel and Kolomiets.<sup>14</sup> Those measurements were made on bulk samples quenched from the melt, the highest concentration of  $\text{As}_2\text{Te}_3$  apparently being governed by the tendency of the glasses to devitrify if the concentration of  $\text{As}_2\text{Te}_3$  exceeded approximately 70%. Unfortunately, neither the resistivity nor the activation energy are linear functions of composition, so that extrapolation of data to pure  $\text{As}_2\text{Te}_3$  is somewhat difficult, but our values agree within the uncertainty of the extrapolation with the extrapolated values (Fig. 3).

### C. Optical Absorption and Refractive Index

Figure 4 shows the measured optical absorption constants versus photon energy in the spectral region between 1.0 and 1.6 eV. Spectra were measured at the

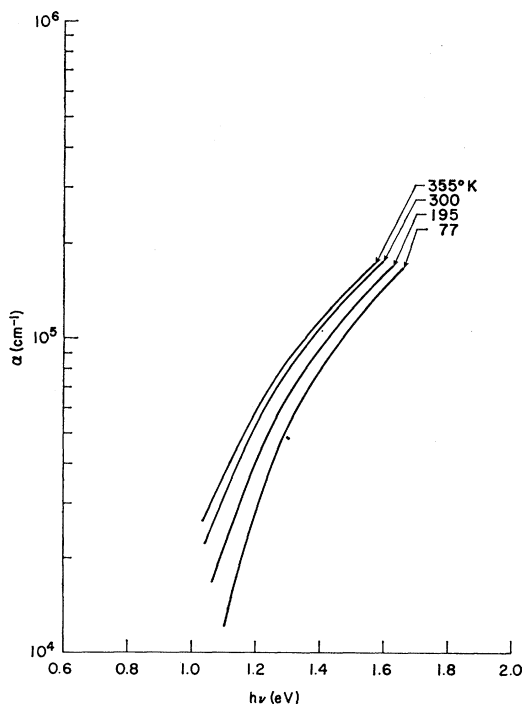


Fig. 4. Absorption constants versus photon energy for 4 temperatures.

TABLE I. Comparison of results for the index of refraction of amorphous  $\text{As}_2\text{Te}_3$  with values extrapolated from measurements on  $\text{As}_2\text{Se}_3\text{-As}_2\text{Te}_3$  alloys.

Temperature (°K)	Present results $\lambda = 1.9 \mu\text{m}$	Hilton <i>et al.</i> <sup>a</sup> $\lambda = 5 \mu\text{m}$	Kolomiets <sup>b</sup> ( $\lambda$ unspecified; see text)
77	3.62		
195	3.70		
300	3.76	3.58	4.73
380	3.80		

<sup>a</sup> Reference 30.

<sup>b</sup> Reference 11.

temperature shown by Pettit. The absorption constant  $\alpha$  at each photon energy was calculated from the optical transmission  $T$  measured with a Cary 14 double-beam spectrophotometer. We used the following expression<sup>28</sup> to relate  $\alpha$  to  $T$ :

$$T = \frac{(1-R_1)(1-R_2)(1-R_3)e^{-\alpha t}}{(1-R_2R_3)\{1-[R_1R_2+R_1R_3(1-R_2)^2]e^{-2\alpha t}\}} \quad (1)$$

Equation (1) applies to the case of an absorbing film of thickness  $t$  on a nonabsorbing substrate. Multiple reflections are included, but coherence and interference effects between reflections are not.  $R_1$ ,  $R_2$ , and  $R_3$  are, respectively, the interface reflectances at the air-film, film-substrate, and substrate-air boundaries. The computation of  $\alpha$  from Eq. (1) requires knowledge of the reflection losses. To estimate these reflection losses, we used the measured index of refraction of the film at a wavelength of  $1.9 \mu\text{m}$  (see below) and the known index of the sapphire substrate. At shorter wavelengths (where  $T \ll 1$ ), Eq. (1) is less sensitive to the exact values of the reflectances and no substantial error is introduced by use of the same reflectances throughout the spectral range considered. In the region where the data overlap, our room-temperature spectrum agrees with Rockstad's results.<sup>25</sup>

Interference fringes were observed in the high-transmission region of the spectra. Indices of refraction were determined from the condition for maximum and minimum transmission.<sup>29</sup> The accuracy of the determination was limited to  $\pm 10\%$  by the accuracy of the film thickness measurements. Table I compares our results on the index of refraction for amorphous  $\text{As}_2\text{Te}_3$  with the extrapolated values reported by Hilton, Jones, and Brau<sup>30</sup> and by Kolomiets,<sup>11</sup> based on measurements of  $\text{As}_2\text{Se}_3\text{-As}_2\text{Te}_3$  amorphous alloys. Our value agrees within experimental error with that of Hilton, Jones, and Brau's, but is significantly lower than the value obtained by Kolomiets. Kolomiets's refractive indices probably refer to low-frequency capacitance measurements (al-

<sup>28</sup> R. Tsu, W. E. Howard, and L. Esaki, Phys. Rev. **172**, 779 (1968).

<sup>29</sup> M. Born and E. Wolff, *Principles of Optics* (Pergamon Press, Inc., New York, 1959), Chap. VII.

<sup>30</sup> A. R. Hilton, C. E. Jones, and M. Brau, Phys. Chem. Glasses **7**, 105 (1966).

though this is not explicitly stated in Ref. 11) and therefore the difference probably arises from the infrared reststrahlen absorption bands. Although we are not aware of any reported reststrahlen results for amorphous  $\text{As}_2\text{Te}_3$ , Felty, Lucovsky, and Myers<sup>31</sup> have reported that amorphous  $\text{As}_2\text{S}_3$  and  $\text{As}_2\text{Se}_3$  do show broad reststrahlen reflections.

#### D. Photoconductivity

The photoconductivity was studied by illuminating the sample with repetitive light pulses and measuring the ac voltage developed across a resistor in series with the sample and a battery. Different methods of illumination, amplification, and integration were used as described below. For investigations of the response time of the system, care was taken to choose a series resistor small enough so that the response time measured did not reflect the RC time of the measuring circuit.

The spectral dependence of the photoconductivity was obtained by illuminating the sample with radiation from a globar source passed through a Perkin-Elmer model-98 monochromator. The light was mechanically chopped and the signal was synchronously detected by means of a PAR "lock-in amplifier" triggered from the chopper. The signal was found to be linear with electric field, which was kept below 1000 V/cm, and with light intensity. The results, plotted as change in conductivity per incident photon versus energy, are shown in Fig. 5 for a typical sample. The apparent shoulder in Fig. 5 is the result of an interference fringe; its position varies for samples of different thicknesses, and, therefore, no special significance should be attributed to it.

In order to determine the absolute photoconductivity  $\Delta\sigma/I_0$ , where  $I_0$  is the photon flux per unit area, a calibrated He-Ne laser was used to illuminate the sample. To find  $I_0$ , the laser beam diameter was determined by scanning the beam across a sample of known distance between contacts. From the extent of the flat response

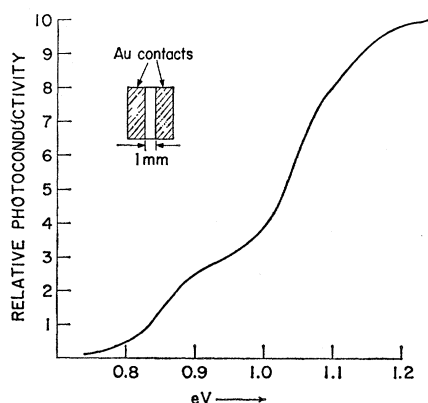


Fig. 5. Normalized photoconductive signal versus photon energy.

<sup>31</sup> E. J. Felty, G. Lucovsky, and M. B. Myers, *Solid State Commun.* **5**, 555 (1967).

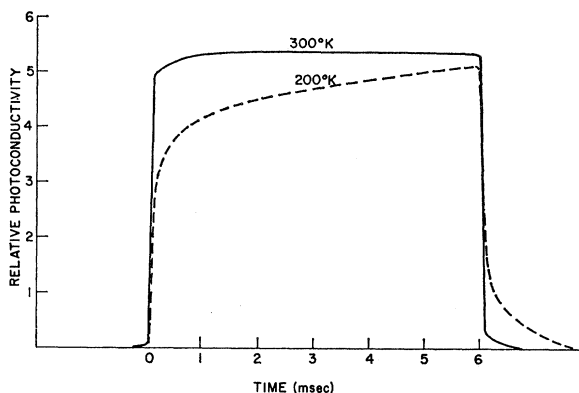


Fig. 6. Relative photoconductive signals versus time using chopped light from a He-Ne laser. The room-temperature response (upper curve) is faster than shown and reflects the light pulse rise time which was limited by the chopper speed.

of the photosignal as the beam was transversed, the diameter was found to be  $0.9 \pm 0.1$  mm. The laser intensity was measured by means of a calibrated Epley thermopile and was found to be 1 mW. In Fig. 6, we show plots of photoconductive signal versus time taken at room temperature and 200°K. The initial room-temperature response time was limited by the chopper speed; as discussed below, the sample response time is considerably faster. At 200°K, however, the response time of the photosignal is seen to be much longer, indicative of trapping effects discussed in Sec. III. Note, however, that even at room temperature a long time constant decay exists.

To determine the actual response time at room temperature, it was necessary to use a much faster rising light pulse than could be obtained by increasing the chopper speed. For this purpose we used a GaAs laser operated at 77°K. The laser was operated at 100 pulses per second at a current of about 2 A and produced approximately 100 mW of power at one end. Using a fast detector, the rise time of the light pulse was found to be less than 10 nsec. The waveform shown in Fig. 7 was obtained by amplifying the signal across a 500- $\Omega$  resistor in series with the sample by means of a Keithley model-110 pulse amplifier. The output from the amplifier was processed with a PAR box car integrator. The trace shown in Fig. 7 was obtained with a gate of 10 nsec. Care was taken to employ a long enough time constant and sweep time to reproduce the waveform faithfully.

### III. DISCUSSION OF RESULTS

#### A. Optical and Conductivity Energy Gaps

Two of the measurements described in Sec. II yield characteristic energies. From the temperature dependence of the conductivity, we find the existence of a "conductivity gap" and from the optical absorption data we shall derive an "optical gap." The data on the

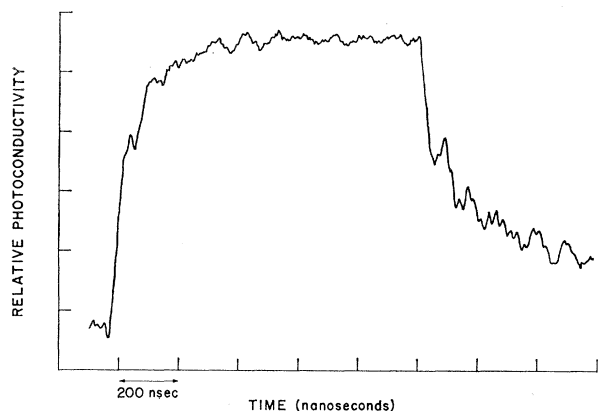


FIG. 7. Room-temperature photoconductivity signal versus time using a pulsed GaAs laser as light source. Rise time of light pulse was approximately 10 nsec.

spectral response of the photoconductivity do not yield any sharp thresholds, and, indeed, one does not expect such an effect with the density-of-states model of Fig. 1. On the basis of such a model, one would expect photoconductivity to set in with photons of essentially zero energy since there are a finite number of states to which electrons and holes can be excited at infinitesimal energy increments above and below the Fermi level. Of course, one would expect the photoconductivity from low-energy photons to be extremely small since the states within the pseudogap are localized and hence electrons in them have a small mobility. As the energy of the photons increases, carriers are promoted into higher energy states of greater mobility, and, thus, the photoconductivity per absorbed photon will increase. Thus, the photoconductivity would gradually increase with energy but no abrupt onset for the photoconductivity will exist, and, indeed, none is seen in Fig. 5.

### 1. Optical Gap

We shall first discuss the derivation and implication of the optical gap obtained from the optical absorption measurements. At first glance, it would seem that by an argument similar to that made for the photoconductivity, no sharp absorption edges in the optical absorption spectrum can be expected. Indeed, Edmond's absorption spectra,<sup>17,32</sup> obtained with thick samples of  $\text{As}_2\text{Se}_3$ - $\text{As}_2\text{Te}_3$  glasses, and Rockstad's spectrum<sup>25</sup> on  $\text{As}_2\text{Te}_3$  films show exponential tails for absorption constants below  $10^4 \text{ cm}^{-1}$ . We have found, nevertheless, that we could treat our high-energy absorption data for amorphous  $\text{As}_2\text{Te}_3$  films in a manner which yields a characteristic optical gap.

<sup>32</sup> Belle, Kolomiets, and Pavlov (Ref. 13) show absorption curves for glassy  $\text{As}_2\text{Se}_3$  for even lower absorption constants than Edmond's. We feel, however, that their range of  $\alpha$ 's is too small for a meaningful interpretation of the data. Furthermore, Edmond points out that the  $\alpha$ 's obtained in this absorption range depend on details of sample preparation.

Figure 8 shows the optical absorption data of Fig. 2 replotted to illustrate that, in the observable spectral range of  $\alpha > 10^4$ , there is a remarkably close fit to the expression

$$\alpha \propto (h\nu - E_G^T)^2 / h\nu, \quad (2)$$

where  $E_G^T$  is the optical energy gap at a temperature  $T$ . Each  $E_G^T$  is found by extrapolation of the plot of  $(\alpha)^{1/2}(h\nu)^{1/2}$  versus  $E$  to zero absorption for each temperature considered. (A similar fit to the absorption data of amorphous GeTe for  $\alpha > 10^4$  has been observed by Howard and Tsu.<sup>33</sup>)

A relation of the form of Eq. (2) can be derived<sup>34</sup> by considering the general form for the absorption constant for photon energy  $h\nu$  due to transitions between a full valence band with density distributions  $g_v$  and an empty conduction band with density distribution  $g_c$ :

$$\alpha = \frac{A'M^2}{h\nu} \int g_c(E')g_v(E'-h\nu)dE', \quad (3)$$

where  $A'$  is a constant and  $M$  is the matrix element for the optical absorption transition to a final state  $E'$ . This equation assumes that all transitions are equally likely, that is, the matrix element is the same for all transitions and that there are no selection rules other than energy conservation.

One obtains Eq. (2) by integrating Eq. (3) over all states  $E'$  connected by the photon energy  $h\nu$ , provided that the states have a parabolic density dependence on  $E$ , i.e.,  $g_c(E) \propto (E')^{1/2}$  and  $g_v(E'-h\nu) \propto (h\nu - E' - E_G^T)^{1/2}$ .  $E_G^T$  is the width of the zero density region between the two bands characterized by the density-of-states functions  $g_v$  and  $g_c$  at the temperature  $T$ . We are now in a position to examine the significance of the good fit of the data to Eq. (2).

A plausible interpretation is that at these energies the densities of states in the valence and conduction bands are parabolic as would be the case in a periodic lattice near the band extreme. This result is certainly not surprising since energetic carriers, i.e., carriers well away from the pseudogap, are not affected strongly by long-range fluctuations of the potential. Therefore, the difference between the amorphous and the crystalline states should not be very significant for such carriers. A justification for the existence of constant matrix elements and of the breakdown of selection rules cannot, *a priori*, be given. Possibly, phonon-assisted processes and the existence of disorder may account for this behavior. In any case, the good fit of the experimental data to Eq. (2) suggests that this behavior prevails. Otherwise, a good fit would only be obtainable by a fortuitous dependence of the matrix elements and of the selection rules on energy in a manner such that the densities of states appear to have a parabolic dependence on energy.

<sup>33</sup> W. E. Howard and R. Tsu (unpublished).

<sup>34</sup> G. J. Lasher and F. Stern, Phys. Rev. **133**, A553 (1964).

The fact that the fit of the data to Eq. (2) yields an optical gap energy  $E_G^T$  does not mean, of course; that there is an energy range in which there are no states.  $E_G^T$  is the gap which separates the extrapolated limits of bandlike states for which Eq. (2) holds. In the actual material, there are tail states and localized states at lower energies so that the density of states never goes to zero. In Fig. 1, we indicate  $E_G$  in the light of the discussion presented above.

The temperature dependence of the optical energy gap is shown in the insert of Fig. 8. The extrapolated value  $E_G^0$  of the gap at 0°K is 0.98 eV. This value may be somewhat high since the temperature variation of the gaps of most semiconductors decreases appreciably below 77°K. We, therefore, estimate  $E_G^0$  to be between 0.95 and 0.98 eV. Between 77 and 355°K the temperature coefficient  $\beta$  of the optical gap is  $-5 \times 10^{-4}$  eV/gap.

## 2. Conductivity Gap

From the temperature dependence of the conductivity, an activation energy  $\Delta E$  is obtained, which from Fig. 2 is seen to be  $0.40 \pm 0.02$  eV. It is not possible, of course, to decide on the basis of the data whether this activation energy represents the ionization energy of an impurity or defect level, or whether, as in the case of an intrinsic semiconductor, it represents half an energy gap. We shall make the latter assumption, since these films were not intentionally doped and because the model of an amorphous semiconductor of Fig. 1 renders the material relatively insensitive to impurities. Thus,  $\Delta E$  is one-half of an energy conductivity gap designated as  $E_c$  in Fig. 1. Such a gap can arise only if the mobility of carriers changes fairly abruptly at the energies  $E_c^n$  and  $E_c^p$  for electrons and holes, respectively. This conclusion can be seen from the following argument. Let the conductivity contribution of the electrons be given by<sup>5</sup>

$$\sigma = \int_{E_F}^{\infty} g(E) f(E) \mu(E) dE, \quad (4)$$

where  $g(E)$ ,  $f(E)$ , and  $\mu(E)$  are the density of states, the Fermi function, and the mobility, respectively. We now define a conductivity edge  $E_c^n$  as that energy which makes the largest contribution to the integral. Similarly, of course, we can obtain an analogous energy  $E_c^p$  for holes. To account for the constancy of  $E_c^n - E_F$  and  $E_c^p - E_F$  we shall have to assume that the mobility of the carriers rises abruptly at the  $E_c$ 's, in a manner suggested by Cohen, Fritzsche, and Ovshinsky<sup>35</sup>: Below the  $E_c$ 's the mobilities are assumed to be negligible while above the  $E_c$ 's they are assumed to depend only weakly on the energy. If the mobility did not behave at least approximately in this fashion, for example, if it were constant or increased only slightly with increasing energy,

<sup>35</sup> M. H. Cohen, H. Fritzsche, and S. R. Ovshinsky, Phys. Rev. Letters **22**, 1065 (1969).

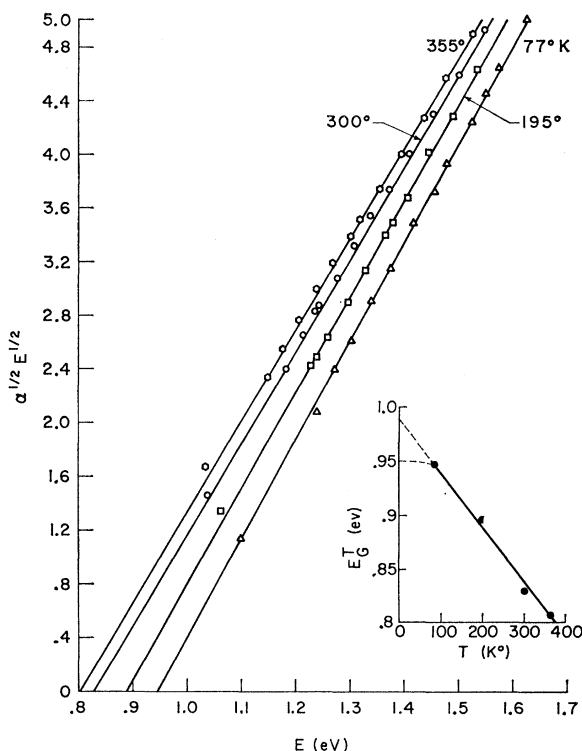


FIG. 8. The function  $(\alpha E)^{1/2}$  versus  $E$  at four different temperatures. The intercepts on the  $E$  axis yield optical energy gaps  $E_G^T$ . The insert shows  $E_G^T$  plotted versus temperature.

the maximum contribution to the integral of Eq. (1) would shift to higher energy with increasing temperature. The reason is that the product  $g(E)f(E)$  exhibits a maximum which moves to higher energies with increasing temperature. If, however,  $f(E)$  is negligible at  $E_c$  and the mobility is negligible below  $E_c$ , then this conductivity edge remains constant with respect to  $E_F$  just as a conduction band edge in an intrinsic crystalline semiconductor remains constant with respect to the Fermi level. The conductivity would then increase exponentially with increasing temperature, following the behavior of the Fermi function for  $E \gg E_F$ . Slight deviations from such an exponential behavior may of course arise from the temperature dependence of the mobility or the density-of-states function.

We, thus, interpret the  $E_c$ 's as "mobility edges" and set the energy difference between them equal to  $0.80 \pm 0.04$  eV from the data of Fig. 2. One would expect  $E_c$  to be similar in magnitude but not identical with the optical gap  $E_G^0$  derived above. It is probable that an abrupt rise in mobility sets in at an energy where the density of localized states becomes comparable to that of delocalized states. Indeed, as discussed below, our estimates of mobility suggests that the carriers at  $E_c$  have a mobility characteristic of "barely" delocalized states which suggests that  $E_c$  represents a border region. The optical gap ( $E_G^0 = 0.95$ – $0.98$  eV), on the other hand,

was derived by means of Eq. (2) whose good fit to the experimental absorption constants suggests that higher-energy states are not only delocalized but actually have a parabolic dependence on energy. One cannot predict, *a priori*, that  $E_G$  should be larger than  $E_c$ . It should be pointed out, however, that this situation is the one found in heavily doped crystalline semiconductors, e.g., Ge. In this case, also conduction takes place at an energy below the conduction band edge.<sup>36</sup>

### B. Mobility of Carriers

With the above interpretation of the conductivity gap  $E_c$  and the assumed behavior of the mobility, it is possible to make an estimate of the mobility of carriers near the  $E_c$ 's from the conductivity data. Another estimate of the mobility can be obtained from measurements of the absolute photoconductivity and of the response time. Over the temperature range investigated the conductivity is of the form  $\sigma = \sigma_0 e^{-\Delta E/kT}$ . In the light of the previous discussion, we set  $\Delta E$  equal to  $E_c/2$ , ( $E_c = 0.8$  eV) and  $\sigma_0$  equal to  $2q\bar{g}\bar{\mu} \exp(\beta/2k)$ , where  $q$  is the electronic charge,  $\bar{g}$  and  $\bar{\mu}$ , respectively, are the effective density of states and the average mobility of carriers near  $E_c^n$  and  $E_c^p$ ,  $\beta$  is the temperature coefficient of  $E_c^n - E_c^p$ , and  $k$  is the Boltzmann constant. The factor of 2 arises from adding the contribution of the carriers at each conductivity edge. In order for  $\sigma$  to depend approximately exponentially on  $1/T$ ,  $\bar{g}$  and  $\bar{\mu}$  must have a negligible dependence on temperature; alternatively the temperature dependence of  $\bar{g}$  and  $\bar{\mu}$  must fortuitously cancel. From Fig. 2, using the average value of  $\sigma$  at room temperature with  $\Delta E = 0.4$  eV, we find  $\sigma_0 = 2q\bar{g}\bar{\mu} \times \exp(\beta/2k) = 600 \Omega^{-1} \text{ cm}^{-1}$ . We use  $\beta = 5 \times 10^{-4}$  eV/deg from the temperature dependence of  $E_G$  (Fig. 8), and, thus, obtain  $\bar{g}\bar{\mu} = 1 \times 10^{20} (\text{cm V sec})^{-1}$ . This choice of  $\beta$  is, of course, only approximate but in view of the similarity between  $E_c (= E_c^n - E_c^p)$  and  $E_G$  it seems quite reasonable. To find  $\bar{\mu}$ , it is clearly necessary to estimate  $\bar{g}$ . If the  $E_c$ 's were simply the band edges in a conventional crystalline semiconductor with effective masses of unity,  $\bar{g}$  at 300°K would be  $2.4 \times 10^{19} \text{ cm}^{-3}$ .<sup>37</sup> The average mobility would then be  $4 \text{ cm}^2/\text{V sec}$  at room temperature. Since, however, the density of states shown in Fig. 1 does not fall off as sharply near  $E_c^n$  and  $E_c^p$  as it does near a band edge in a crystalline semiconductor,  $\bar{g}$  is probably considerably larger than  $2.4 \times 10^{19} \text{ cm}^{-3}$ . One can, however, put an upper limit on  $\bar{g}$  by demanding that the number of states contributing to the conduction process be smaller than the average numbers of states per  $kT$  of the band from which the tail states originate.<sup>38</sup> We estimate the density of the material at  $2.5 \times 10^{22}$  atoms/cm<sup>3</sup>.<sup>30</sup> For a typical band-

width of 4 eV,<sup>39</sup> the average density of states in a range  $kT$  at room temperature is then given by  $2 \times (2.5 \times 10^{22} \text{ cm}^{-3}) \times (kT/4 \text{ eV})$ , or  $3 \times 10^{20} \text{ cm}^{-3}$ ; the factor 2 accounts for the two spin states per electron. We see that  $\bar{\mu}$  would have to be  $0.33 \text{ cm}^2/\text{V sec}$  in order for  $\bar{g}$  to be equal to the average density of states within the band. Since, however, we require  $\bar{g}$  to be smaller than this average, we can assume that  $\bar{\mu}$  is larger than the above value. The uncertainties in the choice of the various parameters used in the above argument ( $\beta$ , width of the band, density, etc.) as well as the limits of error in the experimental data probably introduce factors of order 2 in these estimates. It would appear, however, that  $0.3 \leq \bar{\mu} \leq 5 \text{ cm}^2/\text{V sec}$  which would put the  $E_c$ 's in the borderline region between delocalized and localized states.<sup>1</sup> This situation is just the one to be expected for the mobility to rise abruptly from a negligible value below  $E_c$  to a fairly constant value above  $E_c$ .

Another estimate for the mobility of carriers comes from photoconductivity measurements. In the steady state, a time-independent distribution of excess electrons and holes between all the available levels will be reached. We again assume that only carriers near  $E_c^n$  and  $E_c^p$  contribute appreciably to the conduction process. The photoconductivity will then be given by<sup>40</sup>

$$\Delta\sigma = \eta q (\mu\tau)_{E_c} A I_0 / t h\nu. \quad (5)$$

In this equation,  $\eta$  is the quantum efficiency, i.e., the number of electrons and holes produced per absorbed photon,  $q$  is the electronic charge,  $A$  is the absorptance, and  $t$  is the thickness.  $I_0$  is light flux in energy per cm<sup>2</sup> per sec and  $h\nu$  is the energy per photon, so that  $A I_0 / h\nu t$  is the number of photons absorbed per cm<sup>3</sup> per sec. It is important to realize that the average mobility  $\mu$  and the lifetime  $\tau$  refer to carriers near the mobility edges only. Excess carriers captured by localized states will have a different lower mobility and a different and probably longer lifetime.

For two samples measured at room temperature, we obtained a  $\Delta\sigma$  of  $2 \times 10^{-5} \Omega^{-1} \text{ cm}^{-1}$  with the sample illuminated by the He-Ne laser described in Sec. II. As mentioned above, the laser operated at 1 mW at a wavelength of  $1.15 \mu\text{m}$ , with a beam diameter of 1 mm, so that  $I_0/h\nu$  was  $7.6 \times 10^{17}$  photons/cm<sup>2</sup> sec. Correcting for reflection losses of the Dewar window, we obtain  $I_0/h\nu = 6.5 \times 10^{17}$ . We calculated  $A$  from the relation  $A = 1 - T - R$  where  $T$  is the transmittance and  $R$  the reflectance.  $T$  was taken from the experimental data ( $T = 0.19$  at a wavelength of  $1.15 \mu\text{m}$ ) and  $R$  was the calculated reflectance for the film-substrate structure. The refractive index was taken at 3.76, as indicated in Table I. The absorptance  $A$  was, thus, estimated to be 0.47. Inserting the value for  $t(3800 \text{ \AA})$  into Eq. (5), we find  $(\mu\tau)_{E_c}$  equal to  $1.4 \times 10^{-8} \text{ cm}^2/\text{V}$ .

<sup>36</sup> N. F. Mott and W. D. Twose, *Advan. Phys.* **10**, 107 (1961).

<sup>37</sup> W. Shockley, *Electrons and Holes in Semiconductors* (D. Van Nostrand, Inc., New York, 1950), p. 241.

<sup>38</sup> We are indebted to Professor M. Pollack for clarification on this point.

<sup>39</sup> J. Callaway, *Energy Band Theory of Solids* (Academic Press Inc., New York, 1964), Chap. III.

<sup>40</sup> A. Rose, *Concepts in Photoconductivity and Allied Problems* (Wiley-Interscience, Inc., New York, 1963).



From Fig. 7, we obtain an upper limit for  $\tau$  of approximately  $5 \times 10^{-8}$  sec. The reason this initial rise and fall time of the pulse provides an upper limit for  $\tau$  is that traps which communicate with the conducting state near the  $E_c$ 's within a time of less than  $5 \times 10^{-8}$  sec will slow up the response time.<sup>40</sup> That such traps exist is, of course, borne out by curve b of Fig. 6 which shows their importance at lower temperatures. The higher the temperature the less important the trapping processes, but it is clear from Fig. 6 that traps play a role even at room temperature, as is evident from the long response times after the fast initial rise and fall time. We, therefore, conclude that  $\tau < 5 \times 10^{-8}$  sec, and, with  $\eta = 1$ , it follows that  $\mu > 0.3$  cm<sup>2</sup>/V sec. This value, based on photoconductivity measurements, is consistent with the range of  $\mu$ 's we estimate from the conductivity data, but it should be emphasized again that the photoconductivity data yield only a lower limit.

#### IV. SUMMARY AND CONCLUSIONS

The conductivity of amorphous  $\text{As}_2\text{Te}_3$  films is of the form  $\sigma = \sigma_0 e^{-E/kT}$  with  $\sigma = 600 \Omega^{-1} \text{ cm}^{-1}$  and  $E = 0.40 \pm 0.02$  eV over the temperature range from 200 to 400°K. Interpreting this behavior as being due to an intrinsic amorphous semiconductor we obtain a conductivity energy gap of  $0.80 \pm 0.04$  eV. The edges of this gap are interpreted as the energies at which the electrons and holes make their maximum contribution to the conductivity. It is furthermore argued that the existence of such a gap, independent of temperature, implies the existence of mobility edges, i.e., regions of energy where the mobility of carriers increases quite abruptly from a negligible value to a value which no longer depends strongly on energy.

The optical absorption data in the range of  $10^4 < \alpha < 2 \times 10^5$  cm<sup>-1</sup> were found to depend on energy in a manner which suggests that the absorption in this range

is between bands with densities of states which depend parabolically on energy. Extrapolating the absorption data for these states to zero absorption yields an optical energy gap of  $0.96 \pm 0.02$  eV at 0°K. The significance of this gap is that it would exist, i.e., a region of zero density of states would be present, if these high energy band states were not perturbed by the disorder. The fact that the conductivity gap is less than the optical gap, 0.80 eV compared to 0.96 eV, suggests that the mobility edges are in the border region between delocalized and localized states.

This last conclusion is borne out by our estimates of mobility. We write  $\sigma_0$  as  $q\bar{g}\bar{\mu}e^{\beta/k}$ ; from the temperature dependence of the gap  $\beta$  and the experimental value of  $\sigma_0$ , we estimate the product  $\bar{g}\bar{\mu}$  to be equal to  $2 \times 10^{20}$  cm V sec<sup>-1</sup>. It is then argued that the limits of  $\bar{g}$  are between  $2.4 \times 10^{19}$  and  $3 \times 10^{20}$  cm<sup>-3</sup> so that, approximately,  $\bar{\mu}$  is between 0.3 and 4 cm<sup>2</sup>/V sec. This value is typical of an "almost" delocalized conduction process. From photoconductivity data we conclude that the lifetime of the photocarriers is less than 50 nsec and their mobility is greater than 0.3 cm<sup>2</sup>/V sec. Both our estimates of mobility, from dark conductivity and photoconductivity measurements, are larger than any previously estimated for chalcogenide glasses.<sup>12,18</sup> Our photoconductivity data also indicate the presence of traps as might be expected in an amorphous material.

#### ACKNOWLEDGMENTS

We acknowledge the skillful cooperation of J. A. Reinhold both in the preparation and measurement of samples, and of J. Angilello and Miss E. I. Alessandrin for x-ray and electron diffraction studies. We also thank Professor M. P. Pollak and Dr. F. Stern, Dr. W. Howard, Dr. R. Tsu, and Dr. M. I. Nathan for many enlightening conversations and their critical comments. Finally, we thank G. D. Pettit for taking optical data.